Proc. IEEE Int. Conf. on Robotics and Automation
Minneapolis, MN, April 1996.

A New Measure of Tipover Stability Margin for Mobile Manipulators

E. G. Papadopoulos D. A. Rey
Department of Mechanical Engineering and Center for Intelligent Machines
McGill University
Montréal, Québec H3A 2A7

Abstract

Mobile manipulators operating in field environments will be required to perform tasks on uneven terrain which may cause the system to approach, or achieve, a dangerous tipover instability. To avoid tipover in an automatic system, or to provide a human operator with an indication of proximity to tipover, it is necessary to define a measure of stability margin. This work presents a new tipover stability measure (the Force–Angle stability measure) *which is easily computed and sensitive to topheaviness. The proposed metric is applicable to systems subject to inertial and external forces, operating over even or uneven terrains. Performance of the measure is demonstrated using a forestry vehicle simulation.*

1 Introduction

Mobile machines equipped with manipulator arms and controlled by on-board human operators are commonplace systems in the construction, mining, and forestry industries, see for example Fig. 1. When these systems exert large forces, move heavy payloads, or operate over very uneven or sloped terrain, tipover instabilities may occur which endanger the operator, reduce productivity, and risk damaging the machine. With the introduction of computer control (i.e. a supervisory control system) the safety and productivity of these mobile manipulators could be improved by automatic detection and prevention of tipover instabilities. In order to accomplish this, an appropriate measure of the *tipover stability margin* must be defined. Teleoperated or fully autonomous mobile manipulators operating in field environments (as proposed by the nuclear, military and aerospace industries) would also require a similar monitoring of the tipover stability margin.

Work by the vehicular research community has focused on characterizing the lateral rollover propensity of a vehicle [1, 2, 3]. While the proposed static characterizations of machine lateral stability are not appropriate as instantaneous measures of a vehicle's stability, they do highlight the importance of considering vehicle center-of-gravity (c.g.) height and system mass (i.e. heaviness).

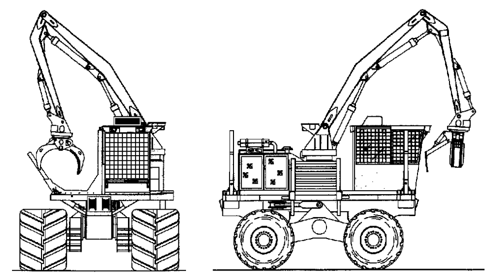

Fig. 1: Example mobile manipulator.

Attempts by the robotics research community to solve the motion planning problem for mobile manipulators travelling over sloped terrain, or exerting large forces or moments on the environment, gave rise to various stability constraint definitions [4, 5, 6]. By considering the degree to which a stability constraint is satisfied, one obtains a measure of the stability margin. However, the proposed measures are not topheavy sensitive and generally only consider lateral tipover.

Several researchers examined more directly the question of how one should define the instantaneous stability margin for a mobile manipulator. McGhee proposed the use of the shortest horizontal distance between the c.g. and the support pattern boundary projected onto a horizontal plane [7, 8]. This measure was refined by Song and later by Sugano, yet it remains insensitive to topheaviness and is only an approximation for systems on uneven terrain [9, 10]. Sreenivasan and Wilcox improve on the minimum distance measure by considering the minimum of each contact point distance to the net force vector, eliminating the need for a projection plane and thereby making the measure exact [11]. However, this measure fails in the presence of angular loads and also does not take into consideration topheaviness. Davidson and Schweitzer also extend the work of McGhee, this time using screw mechanics to provide a measure which eliminates the need for a projection plane while allowing for angular loads [12]. They recognize however that their measure is not sensitive to topheaviness. Messuri and Klein proposed the use of the minimum work required to tipover the vehicle, a measure which is sensitive to c.g. height [13]. Their energy-based approach was extended by

Ghasempoor and Sepheri to include inertial and external loads, subject however to the same assumption of constant load magnitude and direction throughout the tipover motion [14].

This work presents a new tipover stability measure *(the Force–Angle stability measure)* which has a simple graphical interpretation and is more easily computed than the measure of Ghasempoor and Sepheri yet remains sensitive to topheaviness and applicable to the general case of systems operating over uneven terrain and subject to inertial and external forces. The simple nature of the proposed measure and the fact that it does not require any integration make it advantageous to previously proposed measures. Performance of the Force–Angle stability measure is demonstrated using a forestry vehicle simulation.

2 Background

In determining the tipover stability margin of a ground vehicle system, one is necessarily concerned with the stability of the central body which generally provides mobility, i.e. the vehicle body or base. It is assumed in this work that the vehicle body is nominally in contact with the ground, as would be the case if mobility is provided via wheels, tracks, alternating (statically stable) legged support, or a combination thereof. A tipover or rollover instability occurs when a nominally upright vehicle body undergoes a rotation which results in a reduction of the number of ground contact points such that all remaining points lie on a single line (the tipover axis). Mobility control is then lost, and finally, if the situation is not reversed, the vehicle is overturned.

A low c.g. height is always desirable from a stability point-of-view, heaviness on the other hand is stabilizing at low velocities and destabilizing at high velocities. In this work we are concerned with low velocity systems possibly exerting large forces on the environment, hence, heaviness will be considered a stabilizing influence.

3 Force–Angle Stability Measure

To help frame the discussion of the general form of the Force–Angle stability measure we first present a planar example which highlights its simple graphical nature.

3.1 Planar Example

Shown in Figure 2 is a two contact point planar system whose center-of-mass (c.m.) is subject to a net force $\mathbf{f}_r$ which is the sum of all forces acting on the vehicle body except the supporting reaction forces (which do not contribute to a tipover motion instability). This force vector subtends two angles, θ_1 and

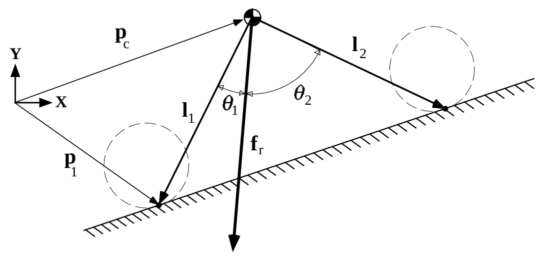

Fig. 2: Planar Force–Angle stability measure.

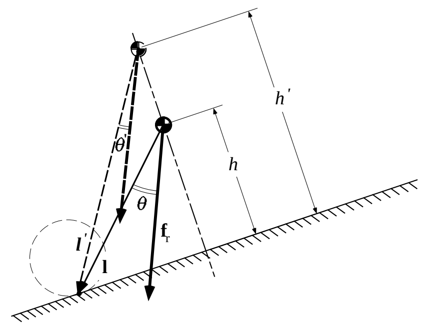

Fig. 3: Effect of center-of-mass height.

θ_2, with the two tip-over axis normals $\mathbf{l}_1$ and $\mathbf{l}_2$. The Force–Angle stability measure, α, is given by the minimum of the two angles, weighted by the magnitude of the force vector (as denoted by $\|\mathbf{f}_r\|$) for heaviness sensitivity:

$$\alpha = \theta_1 \cdot \|\mathbf{f}_r\| \tag{1}$$

Critical tipover stability occurs when θ goes to zero (and therefore $\mathbf{f}_r$ coincides with $\mathbf{l}_1$ or $\mathbf{l}_2$) or, when the magnitude of $\mathbf{f}_r$ goes to zero and even the smallest disturbance may topple the vehicle. If $\mathbf{f}_r$ lies outside the cone described by $\mathbf{l}_1$ and $\mathbf{l}_2$ the angle becomes negative and tipover is in progress. For a vehicle which is capable of adjusting its center-of-mass height, or for a vehicle which carries a variable load, the tipover stability margin should be topheavy sensitive. This is illustrated in Fig. 3 for the Force–Angle stability measure where an increase in c.m. height clearly results in a smaller minimum angle and a reduced measure of tipover stability margin.

3.2 General Form

Geometry

Of all the vehicle contact points with the ground, it is only necessary to consider those outermost points which form a *convex* support polygon when projected onto the horizontal plane. These points will simply be referred to as the ground contact points. Let $\mathbf{p}_i$ represent the location of the i^{th} ground contact point, e.g.

$$\mathbf{p}_i = [\,p_x \;\; p_y \;\; p_z\,]_i^T \qquad i = \{1, \ldots, n\} \tag{2}$$

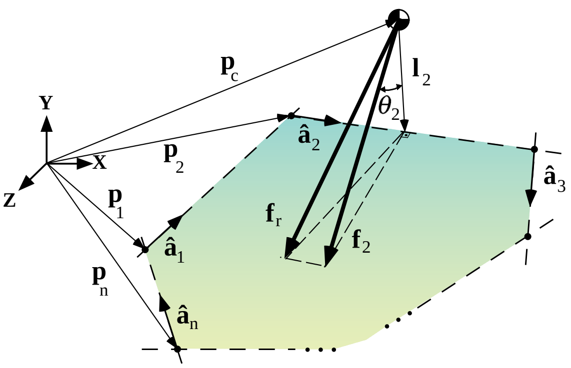

Fig. 4: 3D Force–Angle stability measure.

and let $\mathbf{p}_c$ represent the location of the vehicle center-of-mass. For generality all vectors here are expressed in an inertial frame, although additional simplifications would result from the use of a reference frame located at the vehicle center-of-mass as $\mathbf{p}_c$ would be a zero vector. For a consistent formulation the $\mathbf{p}_i$ are numbered in ascending order following a right-hand rule convention where the thumb is directed downwards along the gravity vector, i.e. points are numbered in clockwise order when viewed from above.

The lines which join the ground contact points are the candidate tipover mode axes, a_i, and the set of these lines will be referred to as the support pattern. The i^{th} tipover mode axis is given by

$$\mathbf{a}_i = \mathbf{p}_{i+1} - \mathbf{p}_i \qquad i = \{1, \ldots, n-1\} \tag{3}$$

$$\mathbf{a}_n = \mathbf{p}_1 - \mathbf{p}_n \tag{4}$$

as shown in Fig. 4. The ground contact point numbering convention was required in order to obtain a set of tipover axes whose directions all coincide with that of *stabilizing* moments.

A natural (i.e. untripped) tipover of the vehicle will always occur about a tipover mode axis a_i. A tripped tipover of the vehicle occurs when one of the ground contact points encounters an obstacle or a sudden change in the ground conditions. In a tripped tipover the vehicle undergoes a rotation about an axis which is some linear combination of the tipover mode axes associated with the single remaining ground contact point. In a tripped instability the Force–Angle stability measure will go to zero and then become negative for each contributing tipover mode axis so that it is not required to identify the exact tipover mode axis. Letting $\hat{\mathbf{a}} = \mathbf{a}/\|\mathbf{a}\|$, the tipover axis normals $\mathbf{l}$ which intersect the vehicle center-of-mass are simply given by subtracting from $(\mathbf{p}_{i+1} - \mathbf{p}_c)$ that portion which lies along $\hat{\mathbf{a}}_i$, i.e.

$$\mathbf{l}_i = \left(\mathbf{1} - \hat{\mathbf{a}}_i \hat{\mathbf{a}}_i^T\right)(\mathbf{p}_{i+1} - \mathbf{p}_c) \tag{5}$$

where $\mathbf{1}$ is the 3x3 identity matrix.

Dynamics

From Newtonian principles we have the following force equilibrium equation for the vehicle body

$$\Sigma\, \mathbf{f}_{\text{inertial}} = \Sigma\left(\mathbf{f}_{\text{grav}} + \mathbf{f}_{\text{manip}} + \mathbf{f}_{\text{support}} + \mathbf{f}_{\text{dist}}\right) \tag{6}$$

where $\mathbf{f}_{\text{inertial}}$ are the inertial forces, $\mathbf{f}_{\text{grav}}$ are the gravitational loads, $\mathbf{f}_{\text{manip}}$ are the loads transmitted by the manipulator to the vehicle body (due to manipulator dynamics, end-effector loading, and end-effector reaction forces), $\mathbf{f}_{\text{support}}$ are the reaction forces of the vehicle support system, and $\mathbf{f}_{\text{dist}}$ are any other external disturbance forces acting directly on the vehicle (e.g. forces due to a trailer implement). Note that in the absence of independent inertias between the vehicle body and the ground we have that the $\mathbf{f}_{\text{support}}$ are equal to the ground reaction forces.

The net force acting on the c.m. that would participate in a tipover instability, $\mathbf{f}_r$, is thus given by

$$\begin{aligned}\mathbf{f}_r &\triangleq \Sigma\left(\mathbf{f}_{\text{grav}} + \mathbf{f}_{\text{manip}} + \mathbf{f}_{\text{dist}} - \mathbf{f}_{\text{inertial}}\right) \\ &= -\Sigma\, \mathbf{f}_{\text{support}}\end{aligned} \tag{7}$$

Similarly, we have for the net moment $\mathbf{n}_r$ acting about the c.m.

$$\begin{aligned}\mathbf{n}_r &\triangleq \Sigma\left(\mathbf{n}_{\text{grav}} + \mathbf{n}_{\text{manip}} + \mathbf{n}_{\text{dist}} - \mathbf{n}_{\text{inertial}}\right) \\ &= -\Sigma\, \mathbf{n}_{\text{support}}\end{aligned} \tag{8}$$

For a given tipover axis $\hat{\mathbf{a}}_i$ we are only concerned with those components of $\mathbf{f}_r$ and $\mathbf{n}_r$ which act *about* the tipover axis, so we let

$$\mathbf{f}_i = \left(\mathbf{1} - \hat{\mathbf{a}}_i \hat{\mathbf{a}}_i^T\right)\mathbf{f}_r \tag{9}$$

and

$$\mathbf{n}_i = \left(\hat{\mathbf{a}}_i \hat{\mathbf{a}}_i^T\right)\mathbf{n}_r \tag{10}$$

Angular Loads

Since the Force–Angle stability measure is based on the computation of the angle between the net *force* vector and each of the tipover axis normals, it is necessary to replace the moment $\mathbf{n}_i$ with an equivalent force couple $\mathbf{f}_{n_i}$ for each tipover axis. The equivalent force couple must necessarily lie in the plane normal to the moment $\mathbf{n}_i$. The most judicious choice of the infinite possible force couple locations and directions in this plane, is that pair of minimum magnitude where one member of the couple passes through the center-of-mass and the other through the line of the tipover axis. As shown in Fig. 5, the member of the force couple acting on the center-of-mass is then given by

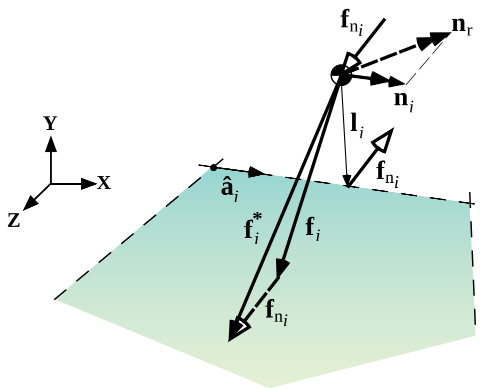

Fig. 5: Use of equivalent force couple to replace moment at c.g.

$$\mathbf{f}_{n_i} = \frac{\hat{\mathbf{l}}_i \times \mathbf{n}_i}{||\mathbf{l}_i||} \tag{11}$$

where $\hat{\mathbf{l}} = \mathbf{l}/\,||\mathbf{l}||$. The new net force vector $\mathbf{f}_i^*$ for the i^{th} tipover axis is thus

$$\mathbf{f}_i^* = \mathbf{f}_i + \frac{\hat{\mathbf{l}}_i \times \mathbf{n}_i}{||\mathbf{l}_i||} \tag{12}$$

Force–Angle Stability Measure

Letting $\hat{\mathbf{f}}^* = \mathbf{f}^*/\,||\mathbf{f}^*||$, the candidate angles for the Force–Angle stability measure are then simply given by

$$\theta_i = \sigma_i \cos^{-1}\left(\hat{\mathbf{f}}_i^* \cdot \hat{\mathbf{l}}_i\right) \qquad i = \{1, \ldots, n\} \tag{13}$$

where $-\pi \leq \theta_i \leq \pi$. The sign of θ_i is determined by σ_i as follows

$$\sigma_i = \begin{cases} +1 & \left(\hat{\mathbf{l}}_i \times \hat{\mathbf{f}}_i^*\right) \cdot \hat{\mathbf{a}}_i < 0 \\ -1 & \text{otherwise} \end{cases} \tag{14}$$

where $i = \{1, \ldots, n\}$. Note that the appropriate sign of the angle measure associated with each tipover axis is determined by establishing whether or not the net force vector lies inside the support pattern.

The overall Force–Angle stability measure is then simply given by

$$\alpha = \min\left(\theta_i\right) ||\mathbf{f}_r|| \qquad i = \{1, \ldots, n\} \tag{15}$$

This scalar is thus an instantaneous measure of the tipover stability margin of the system. The magnitude of a positive α describes the magnitude of the tipover stability margin of a stable system. Critical tipover stability occurs when $\alpha = 0$. Negative values of α indicate that a tipover instability is in progress. Note that the minimum angle is weighted by $||\mathbf{f}_r||$ in order to obtain heaviness sensitivity and not by $||\mathbf{f}_i||$ which would introduce discontinuities in α whenever the tipover axis index i associated with $\min(\theta_i)$ changes.

While this single measure can be used to describe the global tipover stability margin of the system, it is often advantageous to monitor the tipover stability margin measure associated with *each* of the tipover axes, e.g. for use in a display system for a human operated or teleoperated machine. To track the Force–Angle stability measures associated with the i^{th} tipover axis one need simply use

$$\alpha_i = \theta_i\, ||\mathbf{f}_r|| \tag{16}$$

3.3 Requirements

To compute the Force–Angle stability measure one must thus have knowledge of the location of the ground contact points of the vehicle relative to the vehicle center-of-mass location, knowledge of the external forces and moments acting on the vehicle, and knowledge of the vehicle linear and angular accelerations. All of these are necessary elements of any dynamic system simulation, and are all measurable quantities on a real system equipped with an appropriate sensor suite.

4 Applications and Normalisation

Depending on the particular application of the Force–Angle stability measure, various normalisations are appropriate. The three levels of application for such a stability measure are:

i) tipover stability margin monitoring for a *particular* machine in operation or simulation,

ii) tipover stability characterization for comparing various machines in a given weight/size class or application class (e.g. micro-rovers or forestry vehicles),

iii) tipover stability characterization for comparing various machines belonging to different classes.

The level 1 application class includes real-time monitoring (for tipover prediction and prevention) and off-line simulation (for path planning and optimization). When applied to a particular machine in operation, one should normalise the stability measure by its nominal value in order to better condition the computational problem and to facilitate interpretation by a human operator or teleoperator if present, e.g.

$$\hat{\alpha}_i = \frac{\theta_i}{\theta_{i_{\text{nom}}}} \left\| \frac{\mathbf{f}_r}{\mathbf{f}_{\text{grav}_{\text{nom}}}} \right\| \tag{17}$$

where $\theta_{i_{\text{nom}}}$ and $\mathbf{f}_{\text{grav}_{\text{nom}}}$ are the nominal values for θ_i and $\mathbf{f}_{\text{grav}}$ for the system on a level surface with the arm in home position. For the level 2 case, one should consider using both the unnormalised Force–Angle stability measure, and the measure normalised by the nominal and/or maximum operating loads (inertial and external). While each of these measures predicts the same critical stability point, together they provide a more revealing profile of machine stability than a single characterization. For the level 3 case, where the machines belong to different classes, one must normalise by the nominal or maximum operating loads for a meaningful comparison.

5 Example

The Force–Angle stability measure was implemented in a planar simulation of a mobile manipulator with fundamental characteristics similar to that of the forestry vehicle of Fig. 1. The longitudinal plane model captures inertial effects, external loading effects, tire slip and compliance. Manipulator masses are assumed lumped at the joints. Key system parameters are listed in Table 1.

Table 1: System parameters

	mass [kg]	length [m]	mom. of inertia [kgm^2]
vehicle	10,000	–	10,000
link 1	500	3.5	500
link 2	500	3.5	500
tool	1000	–	4000
vehicle c.m. position [m]			$\mathbf{p}_c = [\ 0.00,\ 0,\ \ 0.00]^T$
front wheel hub position [m]			$\mathbf{p}_1 = [\ 1.50,\ 0, -0.25]^T$
rear wheel hub position [m]			$\mathbf{p}_2 = [-0.50,\ 0, -0.25]^T$
manipulator base position [m]			$\mathbf{p}_b = [\ 0.50,\ 0,\ \ 0.50]^T$
undeformed tire radii [m]			$r_{\text{und}} = 0.65$

The seven generalized coordinates of the system are the three vehicle inertial pose coordinates (i.e vehicle center-of-mass position (x_v, y_v), and vehicle pitch angle (θ_z)) the two wheel angular positions, (θ_i), and the two manipulator joint angles, (ϑ_i), so we have

$$\boldsymbol{q} = [\ x_v,\ y_v,\ \theta_z \mid \theta_1,\ \theta_2 \mid \vartheta_1,\ \vartheta_2]^T \tag{18}$$

The associated vector of generalized input forces is of the form,

$$\boldsymbol{\tau} = [\ \mathbf{0}^T \mid \boldsymbol{\tau}_w^T \mid \boldsymbol{\tau}_m^T\ ]^T \tag{19}$$

The only external wrenches of importance on the system are assumed to be the ground forces for each tire in contact with the ground, and the reaction wrench, if any, at the end-effector. A Dugoff tire force element model [15] was used to model slip. Enhancements were made to the model to account for the special cases of wheel hop or lift-off, locked wheels, backsliding, and reverse direction motion. The slip model prescribes the longitudinal forces at the tire contact patches, while the normal reaction force is prescribed by the tire compliance model.

Sample Task

The sample task used here to demonstrate a possible evolution of the Force–Angle stability measure has four principal phases: i) the system is initially at rest with locked wheels on an inclined surface of 5°, ii) the manipulator is commanded to reach forward and downward, iii) a heavy object (750 kg) is picked-up, and iv) the arm over-extends forward while carrying the object and a tipover instability is initiated. To highlight the sensitivity of the Force–Angle measure to variations in base loading and c.m. height, two additional cases are studied where the same sample task is performed. In one case the vehicle is initially loaded with 7500 kg (e.g. of logs or construction material) and the resulting increase in center-of-mass height is 0.5 m. In the second hypothetical case the center-of-mass is again raised by 0.5 m but without an associated increase in the mass of the base.

Results

Presented in Fig. 6 is the time history of the normalised Force–Angle stability margin measure, $\hat{\alpha}$, for all three cases, and presented in Fig. 7 for reference purposes are the manipulator joint angle time histories and the prescribed end-effector tip load time history.

Since the c.m. of the vehicle is nominally rearward, the normalised tipover stability margin is greater than unity for the platform on the −5° slope. As the arm reaches forward the optimal Force–Angle is achieved and the stability margin reaches a peak. At this point, the principal tipover axis switches from the rear axis to the front axis. As the arm reaches further forward, the tipover stability margin is progressively reduced. Similarly, when the arm picks up the tip load of 750 kg we see a further important reduction in the tipover stability margin. If the base is not displaced and the arm is used to move the load forward, the tipover stability margin goes to zero and becomes negative as the vehicle tips forward.

By monitoring the Force–Angle stability margin an operator or an autonomous system would certainly have adopted the more suitable technique of displacing the load forward by moving it closer to the vehicle and using simultaneous or subsequent forward motion of the platform.

For the case of the loaded vehicle with the raised center-of-mass we see that the effect of the increased heaviness is more important than the effect of the raised center-of-mass as the tipover stability margin

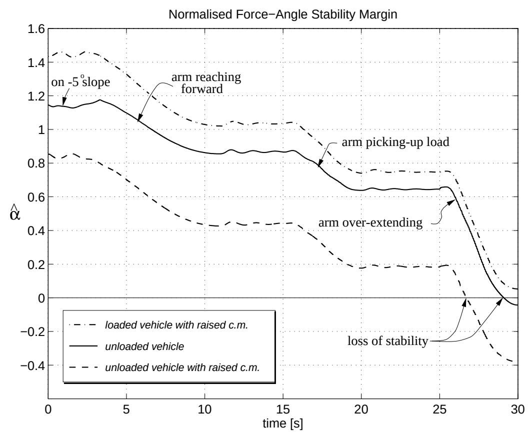

Fig. 6: Force–Angle stability measure for sample task.

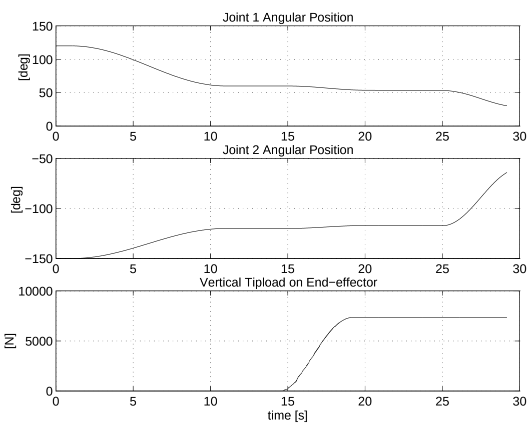

Fig. 7: Joint angles and tip load for sample task.

is increased rather than decreased. The increased stability due to the increased mass of the base is sufficient in fact to prevent the tip-over instability from occuring at the end of the tip load displacement. For the case of the vehicle with a raised center-of-mass without an associated increase in mass, the Force–Angle tipover stability measure is reduced and as expected the tipover instability occurs sooner than for the other more stable cases.

6 Conclusions

This work presented a new tipover stability measure, *the Force–Angle stability measure,* which is sensitive to topheaviness and is applicable to dynamic systems subject to inertial loads and external forces. The proposed measure has a simple geometric interpretation and ease of computation not found in other comparable metrics proposed to date. The three various possible application classes for such a tipover stability margin measure were presented along with recommended normalisations. Performance of the measure was demonstrated using a forestry vehicle simulation.

Acknowledgements

The support of this work by the IRIS–2 Centres of Excellence (ISDE-4) and by the McGill Faculty of Graduate Studies and Research is gratefully acknowledged.

References

[1] I. S. Jones and M. B. Penny, "Engineering parameters related to rollover frequency," *SAE Trans.*, no. 900104, 1990.

[2] W. Buchele and L. Xie, "Computer analysis of the lateral stability of agricultural tractors," in *Amer. Society of Agricultural Eng. Winter Meeting*, no. 901589, 1990.

[3] J. W. Blakenship, K. H. Means, and C. J. Biller, "Side slopes static stability of double–articulated logging tractor," *SAE Trans.*, no. 841140, 1984.

[4] Y. Li and A. A. Frank, "A moving base robot," in *Proc. of American Control Conference*, (Seattle, WA), pp. 1927–1932, June 1986.

[5] S. Dubowsky and E. E. Vance, "Planning mobile manipulator motions considering vehicle dynamic stability constraints," in *IEEE Int. Conf. on Robotics and Automation*, (Scottsdale, AZ), pp. 1271–1276, May 1989.

[6] Z. Shiller and Y.-R. Gwo, "Dynamic motion planning of autonomous vehicles," *IEEE Trans. on Robotics and Automation*, vol. 7, pp. 241–249, Apr. 1991.

[7] R. B. McGhee and A. A. Frank, "On the stability properties of quadruped creeping gait," *Mathematical Biosciences*, vol. 3, no. 2, pp. 331–351, 1968.

[8] R. B. McGhee and G. I. Iswandhi, "Adaptive locomotion of a multilegged robot over rough terrain," *IEEE Trans. on Systems, Man, and Cybernetics*, vol. SMC-9, no. 4, pp. 176–182, 1979.

[9] S. M. Song and K. Waldron, *Machines that Walk.* Cambridge, MA: MIT Press, 1989.

[10] S. Sugano, Q. Huang, and I. Kato, "Stability criteria in controlling mobile robotic systems," in *IEEE/RSJ Int. Workshop on Intelligent Robots and Systems*, (Yokohama, Japan), pp. 832–838, July 1993.

[11] S. V. Sreenivasan and B. H. Wilcox, "Stability and traction control of an actively actuated micro-rover," *J. of Robotic Systems*, vol. 11, pp. 487–502, Sept. 1994.

[12] J. K. Davidson and G. Schweitzer, "A mechanics-based computer algorithm for displaying the margin of static stability in four-legged vehicles," *Trans. ASME J. Mechanical Design*, vol. 112, pp. 480–487, Dec. 1990.

[13] D. A. Messuri and C. A. Klein, "Automatic body regulation for maintaining stability of a legged vehicle during rough-terrain locomotion," *IEEE J. Robotics and Automation*, vol. RA-1, pp. 132–141, Sept. 1985.

[14] A. Ghasempoor and N. Sepehri, "A measure of machine stability for moving base manipulators," in *IEEE Int. Conf. on Robotics and Automation*, (Nagoya, Japan), pp. 2249–2254, May 1995.

[15] H. Dugoff, P. Fancher, and L. Segel, "An analysis of tire traction properties and their influence on vehicle dynamic performance," *SAE Trans.*, no. 700377, 1970.